J Mater Sci (2009) 44:3600–3607
DOI 10.1007/s10853-009-3487-7

# One-pot synthesis of ordered mesoporous carbon–silica nanocomposites templated by mixed amphiphilic block copolymers

**Y. R. Liu**

Received: 23 February 2009 / Accepted: 10 April 2009 / Published online: 28 April 2009


**Abstract** Mixed amphiphilic block copolymers of poly (ethylene oxide)-poly(propylene oxide)-poly(ethylene oxide) (PEO–PPO–PEO) and polydimethylsiloxane-poly(ethylene oxide) (PDMS–PEO) have been successfully used as co-templates to prepare ordered mesoporous polymer–silica and carbon–silica nanocomposites by using phenolic resol polymer as a carbon precursor via the strategy of evaporation-induced self-assembly (EISA). The ordered mesoporous materials of 2-D hexagonal (*p6m*) mesostructures have been achieved, as confirmed by small-angle X-ray scattering (SAXS), transmission electron microscopy (TEM), and nitrogen-sorption measurements. Experiments show that using PDMS–PEO as co-template can enlarge the pore sizes and reduce the framework shrinkage of the materials without evident effect on the specific surface areas. Ordered mesoporous carbons can then be obtained with large pore sizes of 6.7 nm, pore volumes of 0.52 $cm^3/g$, and high surface areas of 578 $m^2/g$. The mixed micelles formed between the hydrophobic PDMS groups and the PPO chains of the F127 molecules should be responsible for the variation of the pore sizes of the resulting mesoporous materials. Through the study of characteristics of mesoporous carbon and mesoporous silica derived from mother carbon–silica nanocomposites, we think mesoporous carbon–silica nanocomposites with the silica-coating mesostructure can be formed after the pyrolysis of the PDMS–PEO diblock copolymer during surfactant removal process. Such method can be thought as the combination of surfactant removal and silica incorporation into one-step. This simple one-pot route provides a pathway for large-scale convenient synthesis of ordered mesostructured nanocomposite materials.

Y. R. Liu (✉)
Department of Material Science, Faculty of Chemistry and Material Science, Shanxi Normal University, Linfen, Shanxi 041004, People's Republic of China
e-mail: liuyr1978@163.com

## Introduction

Ordered mesoporous silica and carbon with regular frameworks and high surface areas have received much attention because of their potential applications in adsorption, separation, hydrogen-storage, electrode materials, nanodevice, photonic waveguide, encapsulation of proteins and catalysis [1–3]. However, the large structural shrinkage during the pyrolysis and carbonization limits the potential applications of mesoporous silica and carbon materials [4]. Nanocomposites can generate remarkable and complementary properties which cannot be obtained in a single component [5–8]. For example, the incorporation of silica into the mesoporous carbon materials not only results in interesting mesoporous carbon–silica nanocomposites, but also may provide materials with improved thermal, chemical, and mechanical properties [9, 10]. Another implied advantage for the incorporation of a rigid constituent of silica into carbon materials is the effective reduction of framework shrinkage [11], which would facilitate one to prepare carbon–silica nanocomposites with large pore sizes. Further removing silica can lead to large-pore mesoporous carbons [12].

The conventional mesoporous carbon–silica nanocomposites were prepared by the infiltration of carbon precursors into preformed mesoporous silica followed by carbonization [13, 14]. The pore blockage often exists in this method and an extra uneconomic process is necessary to prepare silica frameworks. Another approach to achieve

ordered mesoporous carbon–silica nanocomposites is the direct synthesis of periodic mesoporous organosilicas (PMOs) [15, 16]. PMOs represent a new kind of ordered mesostructures derived from surfactant-templated condensation of bridged bifunctional organosiloxane precursors [17]. Integrating organic groups including methylene, ethane, ethylene, and benzene into inorganic solid pore walls is achieved in one-step, which leaves pore voids and improves the smooth accessibility of functional sites [18, 19]. Nevertheless, the bridged bifunctional organosiloxane precursors make the synthesis uneconomic. Inherent hydrophobic character in high organic-content precursors leads to either a phase separation or disordered materials [20]. Multi-component assembly using inorganic silicate oligomers and organic resol precursors and subsequent carbonization is a facile method to prepare carbon–silica nanocomposites [21, 22]. The final nanocomposites have an interpenetrating framework with "reinforced-concrete"-like structure. However, all these syntheses are based on the complicated sol–gel process and adopt relatively expensive inorganic precursors, such as tetraethoxysilane (TEOS).

Polydimethylsiloxane-poly(ethylene oxide) (PDMS–PEO) block copolymers are nontoxic and environmentally compatible and exhibit properties such as low glass-transition temperatures and very low surface tension [23–25]. Such polymers have many applications including surfactants, lubricants, water repellents, and antifoaming agents [26, 27]. Despite wide and extensive industrial usage, very little information is available in the literature on the fundamental surfactant properties of PDMS–PEO in the synthesis of mesoporous materials. To our knowledge, only three reports on the preparation of mesoporous silica materials using PDMS–PEO block copolymers [28–30] are available.

Here we report a new kind of simple and efficient approach to prepare well-ordered mesoporous polymer–silica and carbon–silica nanocomposites by using resol as a polymer precursor, mixed amphiphilic block copolymers of poly(ethylene oxide)–poly(propylene oxide)–poly(ethylene oxide) (PEO–PPO–PEO) and PDMS–PEO are used as co-templates. In this method, PDMS–PEO diblock copolymer plays a double role. On one hand, PDMS–PEO carrying hydrophilic PEO head groups and hydrophobic PDMS chains are clearly amphiphilic molecules and can be used as a co-structure-directing agent [31–33]. On the other hand, PDMS–PEO diblock copolymer also contributes as a silica source. Upon calcination at high temperature, the organic PEO segments are removed and inorganic PDMS backbones are directly decomposed into inorganic silicas. Therefore, silica component can be introduced through one-step process, the hydrolysis and condensation of silica precursors are escaped, suggesting a controllable preparation for silica-containing hybrid materials. To our knowledge, this is the first report of mixed block copolymer surfactants containing PDMS–PEO block copolymer being used to synthesize ordered mesoporous materials.

## Experimetntal section

### Chemicals

Triblock copolymers Pluronic F127 ($M_w$ = 12,600, $EO_{106}$–$PO_{70}$–$EO_{106}$) was purchased from Acros Corp. PDMS–PEO ($M_w$ = 3,012, $DMS_{32}$–$EO_{20}$) diblock copolymer was purchased from Shenzhen Meryer Chemical Technology Co., LTD. Other chemicals were purchased from Shanghai Chemical Corp. All chemicals were used as received without any further purification. Millipore water was used in all experiments.

### Preparation of resol precursors

The resol precursor ($M_w$ < 500) was prepared according to the literature method [34]. In a typical procedure, 0.61 g of phenol was melted at 40–42 °C in a flask and mixed with 0.13 g of 20 wt% NaOH aqueous solution under stirring. After 10 min, 1.05 g of formalin (37 wt% formaldehyde) was added dropwise below 50 °C. Upon further stirring for 1 h at 70–75 °C, the mixture was cooled to room temperature and the pH value was adjusted to about 7.0 by HCl solution. After water was removed by vacuum evaporation below 50 °C, the final product was dissolved in tetrahydrofuran (THF).

### Synthesis of ordered mesoporous polymer–silica and carbon–silica nanocomposites

In a typical preparation, 1.0 g of triblock copolymer F127 and 0.5 g of diblock copolymer PDMS–PEO were dissolved in 20.0 g of THF and stirred for 10 min at 40 °C to afford a clear solution. Next, 5.0 g of 20 wt% resols' THF solution was added in sequence. After being stirred for 0.5 h, the mixture was transferred into dishes. It took 5–8 h at room temperature to evaporate THF and 24 h at 100 °C in an oven to thermopolymerize. The as-made products, flaxen and transparent films or membranes, were scraped from the dishes and ground into fine powders. Calcination was carried out in a tubular furnace at 350 °C for 3 h and at 900 °C for 2 h under $N_2$ flow to get mesoporous polymer–silica and carbon–silica nanocomposites, respectively, named as MP-CS-8.2. "MP-CS-*x*" denotes the mesoporous polymer–silica and carbon–silica nanocomposite samples, wherein *x* represents the percentage of the silica content in the carbon–silica nanocomposite after 900 °C calcination.

**Table 1** Preparation conditions and composites of the ordered mesostructured polymer–silica and carbon–silica nanocomposites via the EISA method

| Sample | PDMS–PEO | F127 | Resol | Polymer%[a] | $SiO_2$%[a] | C–H–O%[b] | $SiO_2$%[b] |
|---|---|---|---|---|---|---|---|
| MP-CS-0 | 0 | 1.0 | 1.0 | 100 | 0 | 100 | 0 |
| MP-CS-8.2 | 0.5 | 1.0 | 1.0 | 93.6 | 6.4 | 91.8 | 8.2 |
| MP-CS-17.8 | 1.0 | 1.0 | 1.0 | 91.3 | 8.7 | 82.2 | 17.8 |

[a] Polymer% and $SiO_2$% were the mass percentages in the polymer–silica nanocomposites, determined from TG results

[b] C–H–O% and $SiO_2$% were the mass percentages in the carbon–silica nanocomposites, determined from TG results

The heating rate was 1 °C/min below 600 °C and 5 °C/min above 600 °C. The typical samples denoted as MP-CS-8.2 and MP-CS-17.8 are listed in Table 1.

It is noticed that in this one-step process silica is incorporated into the mesoporous carbon materials by including the PDMS–PEO in the original surfactant. Considering the ratio of total surfactant and PF resin, excessive PDMS–PEO diblock copolymers may affect the uniformity and structure of resulting mesoporous materials. Then we cannot introduce too much PDMS–PEO surfactant, so the polymer–silica and carbon–silica nanocomposites prepared in the test have relative lower silica content.

### Synthesis of ordered mesoporous carbon and silica from carbon–silica nanocomposites

After carbon–silica nanocomposites were immersed in 10 wt% HF solutions for 24 h, silicas were removed and mesoporous carbons were left. Calcination at 550 °C for 5 h in air could burn off carbons and generate mesoporous silica materials. The mesoporous pure carbon products were named as MP-C-8.2 and MP-C-17.8, respectively, and the pure silica products were named as MP-S-8.2 and MP-S-17.8, respectively, corresponding to their mother nanocomposites.

### Characterization and measurements

The small-angle X-ray scattering (SAXS) measurements were taken on a Nanostar U small-angle X-ray scattering system (Bruker, Germany) using $CuK_\alpha$ radiation (40 kV, 35 mA). The $d$-spacing values were calculated by the formula $d = 2\pi/q$, and the unit cell parameters were calculated from the formula $a_0 = 2d_{10}/\sqrt{3}$. The Brunauer–Emmett–Teller (BET) method was utilized to calculate the specific surface areas ($S_{BET}$) using adsorption data in a relative pressure range from 0.04 to 0.2. By using the Barrett–Joyner–Halenda (BJH) model, the pore volumes and pore size distributions were derived from the adsorption branches of isotherms, and the total pore volumes ($V$) were estimated from the adsorbed amount at a relative pressure $P/P_0$ of 0.992. Transmission electron microscopy (TEM) experiments were conducted on a JEOL 2011 microscope (Japan) operated at 200 kV. The samples for TEM measurements were suspended in ethanol and supported onto a holey carbon film on a Cu grid. Fourier transform infrared (FT-IR) spectra were collected on Nicolet Fourier spectrophotometer, using KBr pellets of the solid samples.

## Results

Mesostructured polymer–silica and carbon–silica nanocomposites were prepared by using triblock copolymers F127 and diblock copolymer PDMS–PEO as co-surfactants and phenolic resol as organic precursor through an EISA process in THF solution. Physicochemical properties of the mesoporous polymer–silica and carbon–silica nanocomposites and of the corresponding mesoporous silica and carbon frameworks are shown in Table 2. Here, we take the mesoporous nanocomposite MP-CS-8.2 as an example. The as-made products are flaxen membranes without obvious macrophase separation.

The SAXS pattern (Fig. 1) for as-made MP-CS-8.2 shows three well-resolved diffraction peaks, associated with 10, 11, and 20 reflections of 2-D hexagonal symmetry with the space group of *p6m* [35]. After calcination at 350 °C in $N_2$, the product turns brown and yields a more resolved SAXS pattern of ordered 2-D hexagonal mesostructure. The unit cell parameter ($a_0$) is reduced from 15.8 to 14.0 nm upon the calcination, reflecting a 11.4% framework shrinkage. After being heated at 900 °C in $N_2$, the nanocomposite becomes black. The SAXS patterns become less resolved and the diffraction peaks broaden. The $q$ vectors move to higher values, implying a contraction of the framework. The unit cell parameter ($a_0$) is calculated to be 11.2 nm, reflecting a framework shrinkage of 29.1%. It is much smaller than that of C-FDU-15 (41.2%) with the same *p6m* symmetry but without silicates inside the framework after heating treatment at 900 °C. This phenomenon clearly demonstrates that the presence of silica in the nanocomposite can efficiently reduce framework shrinkage as compared to pure polymer [36].

**Table 2** Physicochemical properties of the mesoporous polymer–silica and carbon–silica nanocomposites, and of the corresponding mesoporous silica and carbon frameworks obtained after the removal of carbon and silica, respectively

| Sample name | | $a_o$ (nm) | $S_{BET}$ ($m^2$/g) | $D$ (nm) | $V$ ($cm^3$/g) |
|---|---|---|---|---|---|
| MP-CS-0 | As-made | 14.8 | – | – | – |
| | FDU-15 | 12.1 | 650 | 6.8 | 0.63 |
| | C-FDU-15 | 8.7 | 970 | 2.9 | 0.56 |
| MP-CS-8.2 | As-made | 15.8 | – | – | – |
| | Polymer–silica | 14.0 | 615 | 8.0 | 0.67 |
| | Carbon–silica | 11.2 | 788 | 4.9 | 0.64 |
| MP-C-8.2 | Carbon | 10.9 | 517 | 5.4 | 0.50 |
| MP-S-8.2 | Silica | – | 34 | 14.8 | 0.13 |
| MP-CS-17.8 | As-made | 15.9 | – | – | – |
| | Polymer–silica | 15.8 | 707 | 8.0 | 0.81 |
| | Carbon–silica | 13.7 | 756 | 6.2 | 0.68 |
| MP-C-17.8 | Carbon | 13.5 | 578 | 6. 7 | 0.52 |
| MP-S-17.8 | Silica | – | 69 | 22.6 | 0.33 |

The data of MP-CS-0 (FDU-15) came from ref [12]. $a_0$, the unit cell parameter, was calculated by using the formula $a_0 = 2d_{10}/\sqrt{3}$. $S_{BET}$ is the BET surface area. $D$ is the pore size diameter. $V$ is the total pore volume

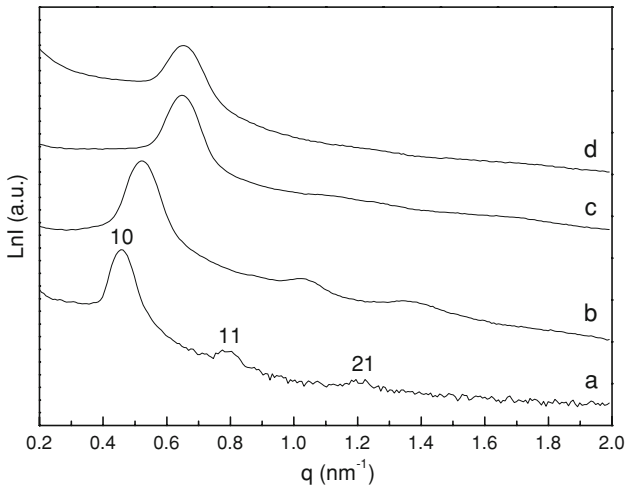


**Fig. 1** SAXS patterns of the mesoporous nanocomposites MP-CS-8.2: (*a*) As-made sample, (*b*) that calcined at 350 °C in $N_2$ (MP-CS-8.2-350 N), (*c*) that calcined at 900 °C in $N_2$ (MP-CS-8.2-900 N), (*d*) MP-C-8.2

The TEM images of MP-CS-8.2-350 N and MP-CS-8.2-900 N, viewed from the [110] and [001] directions together with the corresponding Fourier diffractograms are shown in Fig. 2. The calcined nanocomposites at 350 and 900 °C in $N_2$ show large domains of highly ordered stripe-like and hexagonally arranged images. The results indicate the well-ordered hexagonal arrays of mesopores with 1-D channels of MP-CS-8.2 can be retained after calcination at 900 °C. It further confirms MP-CS-8.2 nanocomposite has a thermally stable *p6m* mesostructure.

Representative TEM images of the mesoporous carbon MP-C-8.2, which was derived from mother nanocomposite MP-CS-8.2 viewed from the [110] and [001] directions, respectively (Fig. 3a, b), further confirm a highly ordered 2-D hexagonal *p6m* mesostructure [35]. TEM images of MP-S-8.2 indicate a disordered mesostructure. It is suggested that the ordered mesostructure cannot be retained after the removal of carbon. The possible reason is that the silica mesostructure has been destroyed during a large amount of carbon combustion, which may leave small residue of silica and many voids.

FT-IR spectra of as-made nanocomposite MP-CS-8.2 (Fig. 4a) show the bands at 2,872 and 1,101 $cm^{-1}$ attributed to the C–H and C–O stretching of triblock copolymer F127 [37] and the overlap with Si–O–Si vibration [38]. A broad band at $\sim$3,410 $cm^{-1}$ and weak band at 1,615 $cm^{-1}$ assigned to the characteristic stretching modes of phenolic resins [39, 40]. The decreasing intensity of bands at around 2,900 $cm^{-1}$ for the nanocomposite calcined at 350 °C in $N_2$ (Fig. 4b) further suggests template decomposition of copolymer F127 [37]. The retained vibrations of phenolic resins and silica indicate the coexistence of polymer and inorganic silica solids. After calcination at 900 °C in $N_2$, the characteristic vibration bands of phenolic resins disappear and those of silicas are retained as shown in FT-IR spectra (Fig. 4c). FT-IR spectrum of mesoporous carbon (Fig. 4e) and silica (Fig. 4d) clearly indicate the framework is composed of carbon and silica, respectively.

$N_2$ sorption isotherms and pore size distribution curves of MP-CS-8.2 and MP-CS-17.8 nanocomposites are shown in Fig. 5, and the corresponding pore characters including BET surface areas, pore volumes, and pore diameters are summarized in Table 2. Ideal $H_1$ hysteresis can be observed for MP-CS-8.2 and MP-CS-17.8 polymer–silica nanocomposites and carbon–silica nanocomposites, suggesting well-ordered cylinder mesopore channels [41]. It is coincident with their highly ordered mesostructures, confirmed by the SAXS and TEM results. All nanocomposites exhibit type-IV curves with distinct capillary condensation steps, suggesting narrow mesopore size distributions [35]. The adsorption and desorption isotherms of mesoporous polymer–silica nanocomposites are not closed at the low relative pressures, which are typical isotherms of polymers [42]. The MP-C-8.2 has a BET surface area of 517 $m^2$/g and a total pore volume of 0.50 $cm^3$/g. A narrow pore size distribution with a mean value of 5.4 nm is calculated from the adsorption branch based on the BJH model. It is larger than the pore size (2.9 nm) of C-FDU-15 with 100% carbon content heated at 900 °C in $N_2$, indicative of a smaller framework shrinkage of the nanocomposite when using PDMS–PEO as co-surfactant. As silica contents increase in

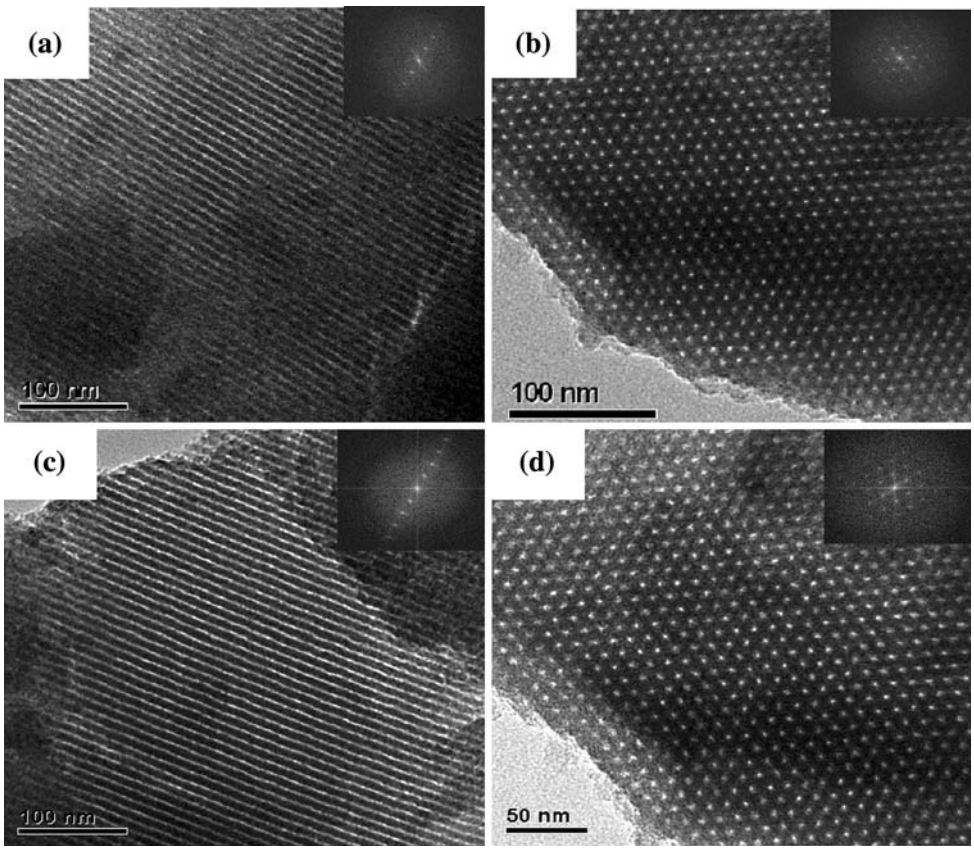


**Fig. 2** TEM images of mesoporous MP-CS-8.2 nanocomposite calcined at 350 °C (**a**, **b**) and 900 °C (**c**, **d**) in $N_2$. The TEM images were recorded along the [110] (**a**, **c**) and [001] (**b**, **d**) directions. The insets are the corresponding FFT diffractograms

carbon–silica nanocomposites, both BET surface areas and pore volumes changes little, while the mean pore sizes gradually enlarge. The mean pore size of MP-C-17.8 remains at a value of about 6.7 nm due to higher silica content and smaller contraction. However, when the silica content is raised, the pore size distribution also becomes wider. This is due to the mesochannels are partially produced by the voids after the removal of silica. Therefore, the pore size distribution is relatively wider than the mother silica–carbon materials. MP-S-8.2 and MP-S-17.8 have very lower BET specific surface areas (34 and 69 $m^2/g$, respectively) and larger calculated pore sizes (14.8 and 22.6 nm, respectively) than their mesoporous carbon counterparts, indicative of a disordered mesostructure. Because the pyrolysis conversion of the PDMS leads to thin discontinuous $SiO_2$ interface layers on the pore wall and that may be destroyed during a large amount of carbon combustion.

Although ordered mesoporous polymer/silica and carbon/silica materials have been synthesized by using mixing templates of different block copolymers, it is clear that such mixing templates strategy just leads to a mono-modal pore system. The main explanation is that the uniform mixed micelles formed in the EISA stages lead to one kind of pore structure. So blocked mesopores or irregular pore windows are not observed from BET results, suggesting silica is coated on the pore wall of mesoporous carbon materials.

## Discussion

The blends of nonionic amphiphiles F127 and PDMS-PEO have been used to direct the formation of high-quality mesoporous carbon–silica nanocomposite materials with two-dimensional (2D) hexagonal mesostructures. On the basis of the above results, we propose that the key controlling factors in the synthesis of ordered mesoporous materials are the compatibility between hydrophilic PEO blocks of both block copolymers and resol precursors. The resol polymers possess plenty of hydroxyl groups, which can form strong hydrogen-bonding interactions with EO-containing block polymers (F127 and PDMS-PEO) and are arranged around block copolymer micelles. The continuous THF evaporation promotes co-assembly of these species and drives the organization of surfactant–resol composites into ordered liquid–crystalline mesophase [43, 44]. The ordered mesophase is solidified, and a nanocomposite with ordered mesostructure can be obtained. Surfactant removal and subsequent carbonization creates ordered mesoporous polymer–silica and carbon–silica nanocomposites, respectively.

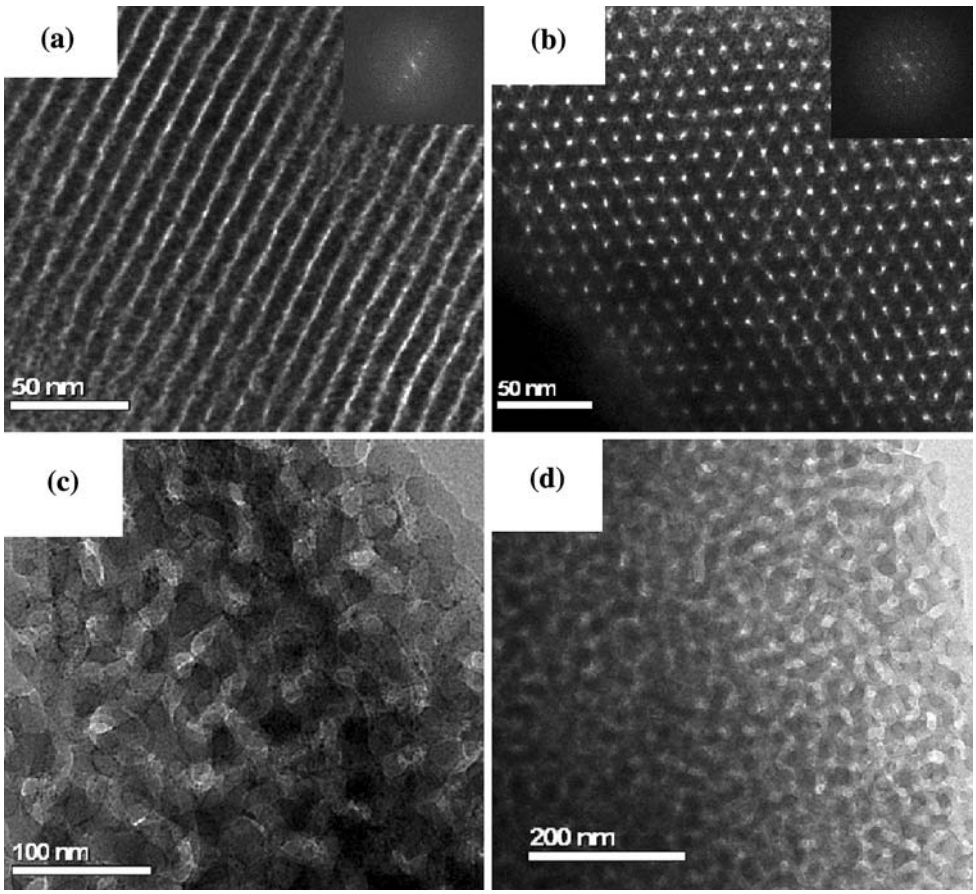


**Fig. 3** TEM images of mesoporous carbon MP-C-8.2 (**a**, **b**) and silica material MP-S-8.2 (**c**, **d**). The TEM images of MP-C-8.2 were recorded along the [110] (**a**) and [001] (**b**) directions. The insets are the corresponding FFT diffractograms

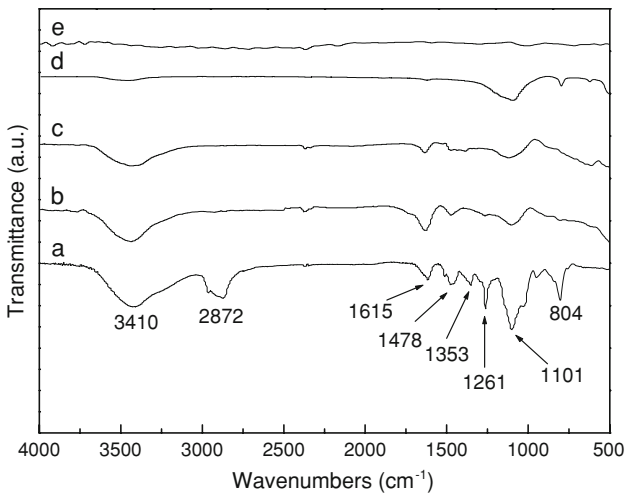


**Fig. 4** FT-IR spectra of MP-CS-8.2 sample. (*a*) As-made MP-CS-8.2, (*b*) that calcined at 350 °C in $N_2$, (*c*) that calcined at 900 °C in $N_2$, (*d*) mesoporous silica, and (*e*) mesoporous carbon

To elucidate the co-template effect of PDMS–PEO on the triblock copolymer F127 templating system, we could analyze the interactions between PDMS–PEO and F127 surfactant. We assume that PDMS–PEO diblock copolymers can interact with F127 surfactant molecules in a more cooperative manner and result in the formation of hybrid micellar aggregates. The mixed micelles could be formed through the van der Waals force and hydrophobic interaction between the hydrophobic PDMS groups and the hydrocarbon tails of the F127 molecules. PDMS–PEO diblock copolymers with hydrophobic PDMS groups can better orient themselves around F127 micelle interface and intercalate these groups to the hydrophobic regions of the F127 micelles during EISA process, which will enlarge the hydrophobic core of F127 surfactant [45, 46]. The outer hydrophilic domains consist of ethylene oxide chains, which form part of the mesopore volume. The PDMS chains cannot penetrate into the core of the micelles formed by Pluronic F127 surfactant, due to the large moiety of hydrophilic EO blocks located on the outer shell of the triblock copolymer F127 micelles. The interconnected segment of PEO blocks facilitates the formation of silica-coating mesostructure after the pyrolysis of the PDMS–PEO diblock copolymer.

In contrast with FDU-15, which is only templated by F127, larger pore sized mesoporous materials may form by using PDMS–PEO block copolymer as co-template. Because PEO–PPO–PEO structure-directing agents with a small difference between the hydrophilicity of the PEO

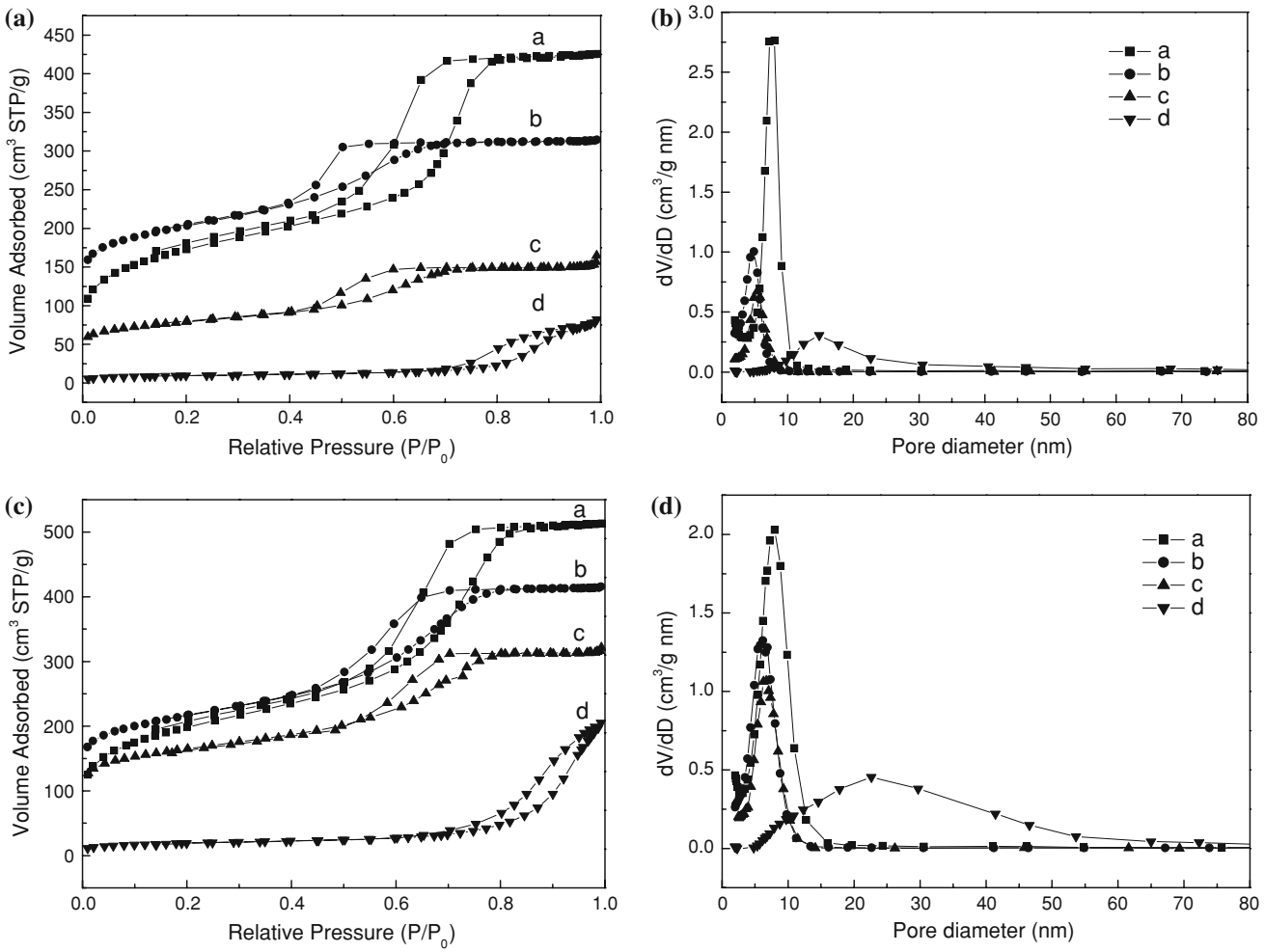


**Fig. 5** $N_2$ sorption isotherms (**a**, **c**) and pore size distribution curves (**b**, **d**) of the mesoporous MP-CS-8.2 (**a**, **b**) and MP-CS-17.8 (**c**, **d**) nanocomposites: **a** calcined at 350 °C, **b** 900 °C in $N_2$, **c** the mesoporous carbon and **d** mesoporous silica products from the mother nanocomposites calcined at 900 °C in $N_2$

block and hydrophobicity of the PPO block are not so effective for forming mesoporous materials with a large amount of PF incorporated. The incorporation of PDMS–PEO increases the hydrophobocity and also leads to an enhanced micro-phase separation. Higher hydrophobicity of PDMS than PPO is believed to be the key factor that influences the swelling of F127 micelles and their further self-assembly behaviors into ordered mesostructures, resulting in an increased pore sized material within the carbon walls. Another important reason is that the pyrolysis of resol polymer is typically accompanied by a decrease in the pore size in as-made materials, and so the frameworks begin to shrink. However, PDMS condensed around micelle templates subsequently results in the protective silica layer upon calcination and reduces this shrinkage to some extent in mesoporous structure.

## Conclusion

We have demonstrated an efficient one-pot approach to synthesize ordered mesoporous polymer–silica and carbon–silica nanocomposites with 2-D hexagonal (*p6m*) mesostructures by using triblock copolymers F127 and diblock copolymer PDMS–PEO as co-templates and phenolic resol as organic precursors through an EISA process. Wherein PDMS–PEO plays three important roles in the synthesis of mesoporous polymer–silica and carbon–silica nanocomposites: (1) as structure-directing agent; (2) as silica source; (3) enlarge the mesopore size and reduce the framework shrinkage. During the process of calcination, the inorganic PDMS segments of PDMS–PEO directly transform to silica. This simple and reproducible one-pot pathway presents several advantages, such as high

modification ratios, homogeneous incorporation, and short preparation times.

Results show that in the presence of rigid silicas the framework shrinkage is reduced, and the pore size of mesoporous carbon is as large as 6.7 nm (MP-C-17.8). The expansion of hydrophobic volume in the amphiphilic F127 triblock copolymers associated with PDMS–PEO copolymers is also attributed to the large pore size of mesoporous materials. Further investigation, however, will be required in order to adequately elucidate the actual formation mechanisms of complex mesophases formed in the mixed surfactant-templating systems containing PDMS–PEO surfactant. Moreover, this simple yet general one-pot route has some special advantages in providing a pathway for large-scale synthesis of ordered mesostructured nanocomposite materials for many potential applications, such as electrode materials, adsorbents, catalyst support, and hydrogen storage, etc.

## References


1. Callone E, Fletcher JM, Carturan G, Raj R (2008) J Mater Sci 43(14):4862. doi:10.1007/s10853-008-2707-x
2. Warren SC, Messina LC, Slaughter LS, Kamperman M, Zhou Q, Gruner SM, Disalvo FJ, Wiesner U (2008) Science 320(5884):1752
3. Jinnai H, Shinbori Y, Kitaoka T, Akutagawa K, Mashita N, Nishi T (2007) Macromolecules 40(18):6758
4. Shen SD, Deng Y, Zhu GB, Mao DS, Wang YH, Wu GS, Li J, Liu XZ, Lu GZ, Zhao DY (2007) J Mater Sci 42(17):7057. doi:10.1007/s10853-007-1608-8
5. Wei Y, Jin DL, Yang CC, Kels MC, Qiu KY (1998) Mater Sci Eng C 6:91
6. Nagarale RK, Gohil GS, Shahi VK, Rangarajan R (2004) Macromolecules 37(26):10023
7. Chen M, Zhou SX, You B, Wu LM (2005) Macromolecules 38(15):6411
8. Scott BJ, Wirnsberger G, Stucky GD (2001) Chem Mater 13(10):3140
9. Wan Y, Min YL, Yu SH (2008) Langmuir 24(9):5024
10. Zhai YP, Tu B, Zhao DY (2009) J Mater Chem 19(1):131
11. Wang ZM, Hohsinoo K, Shishibori K, Kanoh H, Ooi K (2003) Chem Mater 15(15):2926
12. Lee J, Kim J, Lee Y, Yoon S, Oh SM, Hyeon T (2004) Chem Mater 16(17):3323
13. Wang ZM, Shishibori K, Hohsinoo K, Kanoh H, Hirotsu T (2006) Carbon 44(12):2479
14. Choi M, Kleitz F, Liu DN, Lee HY, Ahn WS, Ryoo R (2005) J Am Chem Soc 127(6):1924
15. Asefa T, MacLachan MJ, Coombs N, Ozin GA (1999) Nature 402(6764):867
16. Inagaki S, Guan S, Fukushima Y, Ohsuna T, Terasaki O (1999) J Am Chem Soc 121(41):9611
17. Hunks WJ, Ozin GA (2004) Chem Mater 16(25):5465
18. Yang ZX, Xia YD, Robert M (2006) J Mater Chem 33(16):3417
19. Coutinho D, Gorman B, Ferraris JP, Yang DJ, Balkus KJ (2006) Microporous Mesoporous Mater 91(1–3):276
20. Sayari A, Yang Y (2005) Chem Mater 17(24):6108
21. Hu QY, Kou R, Pang JB, Ward TL, Cai M, Yang ZZ, Lu YF, Tang J (2007) Chem Commun 6:601
22. Liu RL, Shi YF, Meng Y, Zhang FQ, Gu D, Chen ZX, Tu B, Zhao DY (2006) J Am Chem Soc 128(35):11652
23. Haesslin HW, Eicke HF (1984) Makromolekulare Chemie 185:2625
24. Haesslin HW (1985) Makromolekulare Chemie 186:357
25. Zolth KA, Terence C, Brian V (1993) Langmuir 9(5):1258
26. Hewitt DG, Lin J (1998) J Polym Sci Part A Polym Chem 36(7):1093
27. Zhang ZR, Gottlieb M (1999) Thermochimica Acta 336(1):133
28. Xu AW (2002) Chem Mater 14(9):3625
29. Xu AW (2002) J Phys Chem B 106(51):13161
30. Husing N, Launay B, Bauer J, Kickelbick G (2003) J Sol-Gel Sci Technol 26(1–3):609
31. Jan K, Julian C, Chert-Tsun Y, Nicholas AAR, Simon JH (2004) Polymer 45(18):6111
32. Metha R, Paradorn N, Pranee P (2005) Polymer 46(23):9742
33. Guido K, Josef B, Nicola H, Martin A, Krister H (2005) Colloids Surf A Physicochem Eng Asp 254(1–3):37
34. Meng Y, Gu D, Zhang FQ, Shi YF, Yang HF, Li Z, Yu CZ, Tu B, Zhao DY (2005) Angew Chem Int Ed 44(43):7053
35. Zhao DY, Feng JL, Huo QS, Melosh N, Fredrickson GH, Chmelka BF, Stucky GD (1998) Science 279(5350):548
36. Wei Y, Jin DL, Yang CC, Wei G (1996) J Sol-Gel Sci Technol 7(3):191
37. Yang CM, Zibrowius B, Schmidt W, Schuth F (2003) Chem Mater 15(20):3739
38. Sun DH, Zhang R, Liu ZM, Huang Y, Wang Y, He J, Han BX, Yang GY (2005) Macromolecules 38(13):5617
39. Trick KA, Saliba TE (1995) Carbon 33(11):1509
40. Kim J, Lee J, Hyeon T (2004) Carbon 42(12–13):2711
41. Hecht E, Hoffmann H (1994) Langmuir 10(1):86
42. McKeown NB, Budd PM, Msayib KJ, Ghanem BS, Kingston HJ, Tattershall CE, Makhseed S, Reynolds KJ, Fritsch D (2005) Chem Eur J 11(9):2610
43. Wan Y, Yang HF, Zhao DY (2006) Acc Chem Res 39(7):423
44. Grosso D, Cagnol F, Soler-Illia G, Crepaldi EL, Amenitsch H, Brunet-Bruneau A, Bourgeois A, Sanchez C (2004) Adv Funct Mater 14(4):309
45. Almgren M, Vanstam J, Lindblad C, Li PY, Stilbs P, Bahadur P (1991) J Phys Chem 95(14):5677
46. Li Y, Xu R, Couderc S, Bloor DM, Wyn-Jones E, Holzwarth JF (2001) Langmuir 17(1):183